Accelerostat study in conventional and microfluidic bioreactors to assess the key role of residual glucose in the dimorphic transition of Yarrowia lipolytica in response to environmental stimuli

Julie Lesage, Asma Timoumi, Stéphanie Cenard, Eric Lombard, Harry L.T. Lee, Stéphane Guillouet, Nathalie Gorret

Accelerostat study in conventional and microfluidic bioreactors to assess the key role of residual glucose in the dimorphic transition of *Yarrowia lipolytica* in response to environmental stimuli

Julie Lesage[1§], Asma Timoumi[1§], Stéphanie Cenard[1], Eric Lombard[1], Harry L. T. Lee[2], Stéphane E. Guillouet[1] and Nathalie Gorret[1]*

[1]Toulouse Biotechnology Institute (TBI), Université de Toulouse, CNRS, INRA, INSA, 135 Avenue de Rangueil. 35077 Toulouse Cedex, FRANCE

[2]Erbi Bio, Inc, 325 New Boston Stress, Unit 6, Woburn, MA 01801, USA

[§]These authors contributed equally to this work.

* Corresponding author. E-mail: ngorret@insa-toulouse.fr

Abstract

Yarrowia lipolytica, with a diverse array of biotechnological applications, is able to grow as ovoid yeasts or filamentous hyphae depending on environmental conditions. This study has explored the relationship between residual glucose levels and dimorphism in *Y. lipolytica*. Under pH stress conditions, the morphological and physiological characteristics of the yeast were examined during well-controlled accelerostat cultures using both a 1L-laboratory scale and a 1mL-microfluidic bioreactor. The accelerostat mode, via a smooth increase of dilution rate (D), enabled the cell growth rate to increase gradually up to the cell wash-out (D $\geq \mu$max of the strain), which was accompanied by a progressive increase in residual glucose concentration. The results showed that *Y. lipolytica* maintained an ovoid morphology when residual glucose concentration was below a threshold value of around 0.35-0.37mg L^{-1}. Transitions towards more elongated forms were triggered at this threshold and progressively intensified with the increase in residual glucose levels. The effect of cAMP on the dimorphic transition was assessed by the exogenous addition of cAMP and the quantification of its intracellular levels during the accelerostat. cAMP has been reported to be an important mediator of environmental stimuli that inhibit filamentous growth in *Y. lipolytica* by activating the cAMP-PKA regulatory pathway. It was confirmed that the exogenous addition of cAMP inhibited the mycelial morphology of *Y. lipolytica*, even with glucose concentrations exceeding the threshold level. The results suggest that dimorphic responses in *Y. lipolytica* are regulated by sugar signaling pathways, most likely via the cAMP-PKA dependent pathway.

Keywords: accelerostat; residual glucose; cAMP; dimorphic transition; microfluidic bioreactor; *Yarrowia lipolytica*

ABBREVIATIONS

cAMP, cyclic adenosine monophosphate; cAMP-PKA, cAMP-dependent protein kinase; cFDA, carboxyfluorescein diacetate; D, dilution rate (h^{-1}); DO, dissolved oxygen; DCW, dry cell weight; HPLC, haute performance liquid chromatography; HPIC, haute performance ionic chromatography; MAPK, mitogen-activated protein kinase; PDMS, polydimethylsiloxane; PI, propidium iodide

Introduction

The yeast *Yarrowia lipolytica* has generated considerable interest for biotechnological applications due to both its versatility towards carbon source utilization [1-5] and its proficiency in producing a broad spectrum of valuable metabolites [6-11]. Nevertheless, *Y. lipolytica* is known to undergo metabolic and dimorphic transitions in response to environmental fluctuations which can lead to difficulties in scale up of bioprocesses [12].

In previous work [13, 14], the dynamic behavior of *Y. lipolytica* was described in response to pH and dissolved oxygen (DO) fluctuations in well-controlled bioreactor cultures. It was demonstrated that in batch culture, *Y. lipolytica* undergoes dimorphic transition in response to both pH and DO fluctuations. In contrast, *Y. lipolytica* maintains its yeast-like form (ovoid) in chemostat culture conditions at pH7 at all tested dilution rates (from 0.03 h^{-1} to 0.20 h^{-1}), and also at pH5.6 with fluctuations at pH7 [14]. In the case of DO perturbations, chemostat cultures with anoxic periods and at 2 % DO (0.15 mg L^{-1} DO concentration), did not engender mycelial transition. However, filamentation was observed under conditions where limiting O_2 transfer provided only 80% of the cell requirement in the presence of a residual glucose excess. In this particular condition, the system switched from a glucose-limited to an O_2 -limited chemostat culture with an increase in residual glucose concentration and the onset of filamentation [13]. This data suggested a possible impact of residual glucose level on the signaling pathways regulating dimorphic responses in *Y. lipolytica*, but a delayed effect of the onset of O_2 limitation could not be completely ruled out. Indeed, among the rare studies carried out under well-controlled conditions, the effect of a low DO concentration (< 0.13 mg L^{-1}) was evaluated under chemostat at 0.032h^{-1} dilution rate and observed filamentous cells [15] . On increasing the DO concentration, a transition to yeast-like cells was observed. From their results, the authors concluded that there was a direct link between DO limitation and dimorphic transition [15]. As previously described [13], their study was carried out under lipid-producing conditions (N- limitation) and not during the biomass propagation phase. No information on the residual concentration of the C-source was provided, making comparison between the two studies difficult.

It is established that regulation of the dimorphic transition in *Y. lipolytica* is based on the signal transduction pathways involving both mitogen-activated protein kinase (MAPK) and the cyclic-AMP dependent protein kinase A (cAMP-PKA) [16-18]. These pathways operate in opposite directions during the yeast-to-mycelium transition: the MAPK pathway is needed

for mycelial growth while the PKA pathway is required for growth in the yeast-like form [16-18]. Specifically, increasing intracellular cAMP levels inhibited the mycelial growth of *Y. lipolytica* [18, 19]. The cAMP concentration can be increased either by the activation of adenylate cyclase or by the entry of exogenous nucleotides into the cell [18]. Several genes involved in dimorphism have been isolated and characterized, including the Rho family among others. These genes are not only involved in dimorphism, but also in a variety of other cellular activities, such as cell wall organization and biogenesis and membrane trafficking [16, 20-22]. Proteins implicated in the yeast-to-mycelium transition have also been identified and characterized in depth recently in order to unravel the regulatory mechanisms involved in the dimorphic shift [23].

However, to date, a potential relationship between the level of residual glucose and the regulation of the dimorphic transition in *Y. lipolytica* has not been reported and the link between glucose signaling and morphogenesis has only been deciphered for the pathogenic *Candida albicans* [24, 25] and *Saccharomyces cerevisiae* [26, 27]. The glucose-sensing and -signaling mechanisms in yeasts have been well-described, but mainly for *S. cerevisiae*, *Kluyveromyces lactis* and *C. albicans* [28-36], where glucose uptake is a complex process involving different types of transporters and multiple parallel signaling pathways. Three different types of glucose signaling pathways are involved, each playing a distinctive but interacting role: (i) the Rgt2/Snf3 glucose induction pathway, (ii) the Snf1/Mig1, glucose repression pathway, and (iii) the Ras-cAMP-activated kinase (PKA) pathway. Depending on the amount of glucose present in the medium, specific transporters would be expressed and specific signaling pathways induced or repressed. However, in *Y. lipolytica*, sugar assimilation is still poorly understood with only a recent study focusing on the characterization of hexose transporters [37].

Here, the impact of residual glucose concentrations on the induction of the dimorphic transition in response to pH stress has been investigated. In order to modulate the residual glucose concentration under stress conditions, well-controlled accelerostat approaches using a conventional lab-scale reactor and a microfluidic reactor were implemented. The accelerostat strategy was chosen in order to increase gradually the residual glucose concentration in the medium as the dilution rate approached the maximum specific growth rate of the strain (μ_{max}). In addition, the role of cAMP was investigated based on the quantification of intracellular cAMP and the continuous feeding of cAMP during the accelerostat cultures. The dynamic

behavior of *Y. lipolytica* based on quantitative physiological and morphological characterization under accelerostat conditions is reported.

Materials and Methods

Microorganism, media and growth conditions

The strain used was the wild-type *Y. lipolytica* W29 (ATCC® 20460™). Culture conditions and medium composition were performed as previously reported [14]. When necessary, cAMP sodium salt (Sigma-Aldrich, Saint-Quentin Fallavier, France) was dissolved in water, sterilized by filtration and added to the sterile media at a concentration of 25 mM.

Laboratory-scale 1L bioreactor cultures

Batch, glucose-limited continuous and accelerostat cultures were performed in a 1.6 L stainless-steel stirred tank bioreactor with a working volume of 1 L (BIOSTAT® Bplus, Sartorius, Germany) (**Figure 1**A). Reactor equipment and configuration, as well as inoculum preparation steps were as previously described [14]. The temperature was regulated at 28°C and the pH at 5.6 and pH6.5 by addition of 2M KOH (VWR Chemicals, Fontenay-sous-Bois, France). The antifoam polypropylene glycol (PPG) (Sigma-Aldrich, France) was added periodically (pulse-based addition) to maintain a nearly constant concentration (1 mL L^{-1}) in the bioreactor.

Microfluidic 1 mL bioreactor cultures

Perfused, glucose-limited continuous and accelerostat cultures were performed in single-use 1 mL microbioreactor chips (Pharyx Inc., Woburn, MA, USA) (Figure 1B). Detailed description of the design is provided in previous reports [38-40]. The chips were sterilized by γ-radiation (14 KGy). The medium bottles and feed lines were autoclaved separately. The microreactor was equipped with optical density, dissolved oxygen (DO), pH and temperature probes. The growth chamber comprised three interconnected 500 µL sections, of which only two were full at any time to ensure both the 1000µL working volume and the mixing. Gas exchange was ensured by gaseous diffusion across the polydimethylsiloxane (PDMS) membrane. Heating was performed at the base of the device using a resistive heating element. Control and monitoring were performed using MBS_Dashboard software package (Pharyx Inc., Woburn, MA, USA).

Inoculum cultures were prepared as previously described previously [13, 14]. 1 mL of diluted inoculum (5% v/v) was directly injected inside the empty chamber. Temperature was regulated at 28°C. pH was maintained at the set-point (pH5.6 and 6.5) and regulated by addition of 1mM $NaHCO_3$ (Sigma-Aldrich, France) via peristaltic metering valves. Samples for offline analysis were collected via one output port connected to the growth chamber.

Continuous cultivations: chemostat and accelerostat

Continuous cultures were initiated either by batch (1L-bioreactor) or perfusion (microfluidic bioreactor) in order to reach the suitable biomass concentration (≈ 5g L^{-1}). Transitions to continuous mode were carried out at dilution rates (D) of 0.12 h^{-1} and 0.15 h^{-1} for the 1L-laboratory scale bioreactor and the 1mL-microfluidic bioreactor, respectively. Steady-state phases were considered as reached after at least 5 residence times and then characterized during two further residence times.

After characterization of the steady-state phase (D 0.12 h^{-1}/0.15 h^{-1}, pH5.6), the pH was adjusted to 6.5, because at pH7 the medium exhibited slight precipitation. Although the presence of mineral crystals was not an issue in the conventional lab-scale bioreactor, it could be a critical point in the microfluidic device. Indeed, the feed and sampling lines are very thin (1.6 mm internal diameter) and are susceptible to clogging by crystals during fermentation. When the steady-state at pH6.5 and at dilution rate D 0.12 h^{-1}/ 0.15h^{-1} was reached and characterized, the accelerostat phase was launched with an acceleration factor of 0.0025 h^{-1} from D 0.12/ 0.15 to 0.25 h^{-1} (linear increase of dilution rate). Samples were characterized along the steady state and accelerostat phases.

For the study regarding its role, cAMP was added directly in the medium feed solution to a final concentration of 25mM.

Biomass characterization

Biomass concentration

For the 1L bioreactor experiments, the biomass concentration was quantified by spectrophotometric (OD_{620nm}) and dry weight measurements, following the protocol described [14]. For the 1mL microfluidic bioreactor experiments, biomass concentration was quantified spectrophotometrically (OD_{600nm} and OD_{620nm}) using a Nanodrop 1000 spectrophotometer,

(ThermoFisher Scientific, Nanodrop Products, Courtaboeuf, France). This particular instrument has the ability to measure a sample of 1 or 2µl and the pathlength was set at 1mm.

Cell viability and morphology

Cell viability was assessed by flow cytometry following the protocol described previously [14]. Cell morphology was assessed by flow cytometry, morphogranulometry and light microscopy as described [14].

Sugar and organic acid analysis by high-performance liquid chromatography (HPLC) and ionic chromatography (HPIC)

During batch, and perfused phases, glucose and organic acid (acetate, pyruvate, succinate and citrate) concentrations were determined by HPLC as described [14]. Under continuous mode, quantification of glucose and organic acids (acetate, pyruvate, succinate, malate, fumarate and citrate) present at low concentrations in the broth, was carried out by HPIC. All procedures and details of these apparatus were followed according to previously described methods [14].

Cyclic AMP quantification

During chemostat and accelerostat, intracellular cAMP was quantified using the Cyclic AMP Competitive ELISA Kit (Invitrogen, ThermoFisher, Courtaboeuf, France). The acetylated version of the protocol was followed with regard to the intracellular cAMP concentration range encountered. Cell lysates were obtained from samples containing 10^6 cells mL^{-1} treated with 0.1 M HCl (VWR Chemicals, France) as described in the kit protocol.

Gas analysis and monitoring

The online analysis of the inlet and outlet gas compositions for the 1L bioreactor cultivations was performed as described [14]. For the 1mL microfluidic bioreactor, gas analysis was not possible (limit of detection of the equipment).

Calculations

All the calculations (off-gas rates, glucose consumption and biomass production rates and the analysis of cell size distribution at the population level) are described in detail in previously published work [14].

Results

Chemostat – Accelerostat cultures in the 1L lab-scale bioreactor

In order to assess the role of the residual glucose concentration on the onset of the stress response of *Y. lipolytica*, a coupled chemostat/accelerostat approach was implemented. Chemostat cultures were carried out at a selected dilution rate (0.12 h^{-1}) in order to stabilize and characterize the behavior of the cells placed in a steady state. At steady state, the environment being constant, the entire cell population grew at a constant growth rate and exhibited the same physiological state. Subsequently, the accelerostat approach implemented was to gradually increase the cell growth rate up (via the dilution rate) until reaching the cell wash-out ($D \geq \mu max$ of the strain), which consequently led to a gradual increase in glucose availability for cultured cells.

In previous work [14], it was shown that the dilution rate in the tested range (0.03, 0.07, 0.10 and 0.20 h^{-1}) had no impact on the pH stress response of *Y. lipolytica* at pH7. Indeed, under well-controlled chemostat culture at pH7, no filamentation was observed whatever the dilution rate tested, indicating that the growth rate of the cells was not the effector of the dimorphic transition observed during the pH7-batch bioreactor or pH7-pulses batch bioreactor. Thus, the current study was carried out at only one dilution rate ($0.12h^{-1}$).

Chemostat in steady state as a reference

For the chemostat phase, the steady state was considered to be achieved after a period of at least 5 residence times, and was validated by a constant production of biomass and a stable composition of the exhaust gases. Characterization of the steady state at pH6.5 was carried out by taking up at least 7 samples within a period of 2 to 3 residence times. Evolutions of biomass and residual glucose concentrations, as well as changes in pH and DO during this phase are illustrated in **Figure 2**. Constant production of biomass (≈ 4.6 ± 0.2 g L^{-1}) and stable composition of the exhaust gases (19.44±0.04 % O_2, 1.43±0.01 % CO_2 / data not shown) were detected which revealed the stability of the steady state. In addition, negligible amounts of residual glucose (< 5 mg L^{-1}) were quantified in the culture broth, thus confirming the C-limited growth. An O_2 unlimited condition was maintained throughout the chemostat experiments with a DO concentration always > 40%. These results were similar to that previously determined during chemostat cultures of *Y. lipolytica* at pH7 and dilution rate of 0.1 h^{-1} [14].

225 Regarding the macroscopic behavior at the global population scale, specific consumption and
226 production rates, biomass yields as well as C and elemental recoveries were calculated from
227 raw data and reported in **Table 1**. Comparing to results obtained in our previous work [13],
228 the same range of magnitude was obtained, the slight difference being due to the 20%
229 increase of the dilution rate. No production of organic acids was observed. The mean residual
230 glucose concentration was lower than 5mg L^{-1} (Figure 2). Respiratory quotients were around
231 1.1, reflecting the conservation of a fully oxidative metabolism.

232 As previously described [13, 14], the steady state was also characterized at the subpopulation
233 level via cytometry, microscopy and morpho-granulometry measurements. This work
234 confirmed that cells in steady state at pH6.5 were perfectly ovoid-shaped with a unimodal size
235 distribution and a mean cell diameter of about 4.23±0.23 µm. In addition, the viability
236 assessed either by cFDA/PI or cFDA/Sytox double staining methods was maintained >97 %.

237 *Accelerostat*

238 After stabilization and characterization of the steady state, *Y. lipolytica* behavior under
239 glucose-limited chemostat at et and D = 0.12 h^{-1}, the accelerostat approach was implemented
240 to progressively increase the dilution rate up to reaching the cell wash out, which
241 consequently would lead to the increase of residual glucose concentration in the bioreactor.

242 In order to understand the dynamics of morphological changes of *Y. lipolytica* in response to
243 increasing residual glucose concentration, profiles of cell size distribution were analysed
244 regularly during the course of the accelerostat. The width signal of the forward scatter light
245 (FSC), measured by flow cytometry, was used to discriminate subpopulations of different
246 sizes within the culture broth. Number size distributions (**Figure 3A**), based on cell length
247 measurements were determined during the time course of fermentation, and data were
248 displayed as box plots (Figure 3B) illustrating the dispersion and size difference between
249 samples.

250 As shown in Figures 2 and 3, up to a critical dilution rate (D_{crit}) of about 0.19 h^{-1}, where a
251 clear dimorphic transition could be observed, both the macroscopic and microscopic
252 behaviors of cells were similar to those described under steady state conditions. As expected,
253 the increase in the dilution rate above the critical value D_{crit} led to a gradual decrease in the
254 biomass concentration from 4.5 to 3g CDW L^{-1}, which consequently led to an increase in
255 residual glucose from 5mg L^{-1} to 2.5g L^{-1} in the culture broth. At D_{crit}, the residual glucose

concentration was about 0.35g L^{-1}. No organic acids were detected, and cell viability was always >97%. Similarly, for the chemostat, an unlimited O_2 condition was maintained for the entire course of the accelerostat (DO concentration always >40%).

Regarding cell morphology, above the dilution rate of 0.19 h^{-1}, a dispersion of the cell length was observed with a gradual increase in the spread of the distribution of the FSC-Width signal. The time of flight across the laser beam of 95% of the cells increased from 75 to 145 during the accelerostat, while remaining stable around 75 at steady state chemostat and in the accelerostat at D below 0.18 h^{-1} (Figure 3B). This result was confirmed by microscopic observations in real time (Figure 3C). While no filamentation was previously observed at pH7 in glucose-limited chemostat at dilution rates between 0.03 and 0.20 h^{-1} [14], here it has been possible to generate dimorphic transition from yeast to filamentous forms under accelerostat mode at pH7 and under unlimited O_2 condition by increasing the glucose residual concentration.

Chemostat – accelerostat cultures in the 1ml micro-scale bioreactor

A link between cAMP and filamentation has already been described for *Y. lipolytica* [16-19]. In order to identify a more complex interaction between residual glucose concentration, cAMP and dimorphic transition under pH stress conditions, the chemostat-accelerostat approach was carried out using a well-controlled microfluidic bioreactor to be able to continuously supplement with cAMP.

This set of experiments was divided into 4 phases: (i) the steady state chemostat at D = 0.15 h^{-1}, (ii) the accelerostat from 0.15 h^{-1} to 0.25 h^{-1} without cAMP, (iii) a second steady state chemostat at D = 0.15 h^{-1} (data not shown), (iiii) the accelerostat from 0.15 h^{-1} to 0.25 h^{-1} with cAMP. Due to the small volume of the bioreactor and in order to not destabilize the system, only 100µL samples were taken at each time point in order to measure residual glucose and analyze biomass (morphology and viability). pH, DO concentration, and biomass were also on-line monitored (**Figure 4**). As with the 1L-lab scale glucose-limited chemostat culture, a steady state was reached with a stable biomass of about 5 gDW L^{-1}, a stable non-limiting DO concentration (>40%), and a stable residual glucose concentration <1 mg L^{-1} (Figure 4).

Viability was always >97 % and yeast-like cells were largely predominant with a mean diameter of 4.44±0.10µm.

In order to be able to run the complete experiment with the same reactor cassette and to avoid clogging of withdrawal lines with filamentous cells (in the absence of cAMP), the accelerostat with cAMP was carried out first. As shown in **Figure 5**, in the course of the accelerostat, while biomass concentration was decreasing and residual concentration increasing, the yeast cells retained their yeast-like form with an average diameter of about 4.76±0.34 µm (Figure 5A). The time of flight across the laser of 95% of cells was stable at around 80 during the course of the accelerostat (Figure 5B). In contrast, the accelerostat, performed without supplementation of cAMP in the medium, activated dimorphic transition for a residual glucose concentration of about 0.37 g L^{-1} obtained at a D_{crit} of about 0.20 h^{-1}. This D_{crit} value is quite consistent with the results obtained with the 1L bioreactor setup. Without cAMP, a larger size distribution can be observed in the box plot (Figure 4A). To prevent clogging the microfluidic cassette, the filamentation was kept at a lower level (by running shorter time cultivation) than that observed in the lab-scale bioreactor (Figure 5C). In both accelerostat conditions with and without cAMP, the DO concentration was maintained at ~40%, ensuring unlimited O_2 conditions.

cAMP quantification during accelerostat

Quantification of cAMP was carried out in order to evaluate the intracellular level and to compare it between the chemostats and two accelerostat conditions (with or without supplementation of exogenous cAMP in the medium). The results show that under chemostat (steady-state) and accelerostat conditions without cAMP, the intracellular cAMP concentration was below the level of detection of the competitive immunoassay ELISA kit (**Figure 6**). In contrast, it tended to increase progressively during the accelerostat indicating that cAMP was able to enter the cells and consequently may have played a crucial role in inhibiting the dimorphic transition in response to pH stress under glucose excess condition.

Discussion

The objective of this study was to further elucidate the hypothesis of a potential relationship between the level of residual glucose and the dimorphic transition regulation. In order to modulate the residual glucose concentration under stress conditions, well-controlled accelerostat approaches using both classical lab-scale reactor and microfluidic reactor were

implemented. In addition, the role of cAMP was evaluated based on the quantification of intracellular cAMP and the continuous feeding of cAMP during the accelerostat cultures. Dynamic behavior of *Y. lipolitica* based on quantitative physiological and morphological characterizations under accelerostat condition with or without cAMP allowed support for this hypothesis.

In a previous study [14], it was shown that *Y. lipolytica*, considered a model yeast strain for dimorphic transition studies, was able to trigger or not filamentation in response to pH stress depending on the mode of cultivation implemented. Specifically, in batch bioreactors where cells proliferated at their maximum growth rate, mycelia were mainly formed (up to 93% (v/v) at pH7; whereas, in continuous cultures, at controlled growth rates (from 0.03 to 0.20 h^{-1}) even close to the maximum growth rate of the strain (0.24 h^{-1}), only ovoid cell forms were observed. In order to determine whether this behavior was the same under a different stressor (different level of DO concentration), similar experiments have been reported [13]. This set of experiments confirmed that morphological responses of *Y. lipolytica* to various DO levels were also different between batch and chemostat [13]. More specifically, it was suggested that the level of residual glucose in the culture broth might have an impact on the signaling pathways regulating dimorphic transition in *Y. lipolytica*, as the same phenomenon with both stressors pH and DO was observed [13, 14] .

The mechanism of regulation of dimorphic transition of *Y. lipolytica* has been investigated by others [16-18,22,23,41-48]. Those investigations have been mainly carried out in non-controlled batch mode using test-tubes and Erlenmeyer flask cultures except in [47], where chemostat cultures were implemented. Regulation of the dimorphic transition in *Y. lipolytica* was identified as based on the operation of the MAPK and PKA signaling pathways as for other fungi such as *S. cerevisae, C. albicans*, *K. Marxianus, U. maydis* [49, 50]. However, for *Y. lipolytica*, these pathways were shown to operate in opposition during the yeast-to-mycelium transition [45]. The MAPK cascade is involved in mycelial growth whereas an activated PKA pathway is required for growth in the yeast-like form. When inactive, PKA is composed of a heterotetramer of two catalytic subunits (cPKA) attached to a dimer of regulatory PKA subunit (rPKA). When the concentration of intracellular cAMP increases, two molecules of cAMP bind to each rPKa subunit, releasing the catalytic subunit (cPKA) that is then able to phosphorylate target proteins on serine or threonine residues. The intracellular increase in cAMP can be caused either by adenylate cyclase activation or by entry of the exogenous nucleotides into the cell [16-18].

Several genes and proteins have been identified implementing an easier target approach such as specific gene deletion and insertion [16,20,22,45] or global approaches such as proteomic [23] and transcriptomic [45,47] approaches. Based on forward genetic screen and whole-genome sequencing, genes involved in MAPK signaling pathway such as transcription factor Yl*msn2*, the histidine kinase Yl*chk1* and Yl*nik1* as well as the MAP kinase of the of the GOG (high-osmolarity glycerol response) (Yl*ssk2*, Yl*pbs2*, and Yl*hog1)* were identified [47]. Furthermore, they have shown that overexpression of either Yl*mbp1* or Yl*swi6* decreased hyphal growth and deletion of Yl*mbp1* or Yl*swi6* promoted hyphal growth. Nevertheless, despite those molecular studies, the mechanism and effectors of regulation remains unraveled in *Y. lipolytica* unlike for the other yeasts [49].

In addition, the link between glucose sensing pathway and signaling pathway involved in the dimorphic transition have been clearly identified for *S. cerevisae* [26], *C. albicans* [27, 51, 52] and *K. marxianus*. Indeed, different glucose signal pathways are involved depending on the level of glucose in the medium. A simplified scheme has been proposed depicting the sensing and signaling components involved in the induction of the pseudo-hyphal growth by hexose [26]. Two pathways were proposed with glucose as substrate: activation of cAMP-PKA pathway leading to filamentation, and activation of a Glucose/Repression-Induction signaling pathway that would also trigger filamentation via a specific regulator Snf1. Nevertheless, there is no information concerning the level of residual glucose needed for the induction of either pathway. Earlier, it was concluded from another study, that dimorphic transition in *C. albicans* was not regulated by the pH and that glucose or its metabolites may play an important role [51]. Such a result has also been confirmed by [52], showing that glucose starvation led to filamentation under whatever pH condition (neutral or acidic), whereas for unstarved culture (glucose in excess), filamentation was observed only at pH6.7 [52].

No such link between glucose signaling pathway and dimorphic transition signaling pathway has been described in literature for *Y. lipolytica*. Others noticed that a *Y. lipolitica* Δtpk1 mutant, tpk1 coding for the PKA catalytic subunit, showed growth problems when galactose was used as carbon source suggesting a role for PKA in galactose metabolism, although the level of action of PKA remains unknown [16]. Furthermore, there is no description in the literature of the glucose signaling pathway in *Y. lipolytica*. In a recent article, concerning metabolism of alternative substrate metabolism in *Y. lipolytica*, the sugar transporters and mechanism of regulation were discussed based on genome analysis [37] and Blast search, and

it was concluded that the mechanism of regulation is more divergent from those seen in *S. cerevisae,* but without further explanation [53]. Until now, the mechanism of regulation of glucose sensing has remained unclear in *Y. lipolityca* and thereby the link between the glucose sensing and the filamentation. Here it is demonstrated that there is a link between the level of residual glucose and the response to pH stress. As long as the residual glucose was under a certain threshold, only ovoid-yeast cells were present in the culture medium at pH $\geq$ 6.5. As soon as the concentration increased, filamentous cells appeared. Based on those results, it can be concluded that also in *Y. lipolytica*, the level of residual glucose is strongly involved in the signaling response. Such a conclusion has not been reported earlier, probably because of the experimental approaches, based on batch cultures, that have been implemented. Furthermore, it was confirmed that the addition of cAMP could prevent the dimorphic transition even in the presence of a residual glucose concentration. Such effect of cAMP on dimorphic transition has been highlighted earlier [19]. Thanks to the microfluidic bioreactor, it has been possible to carry out a well-controlled accelerostat with a continuous feeding of cAMP at a lower cost, and to observe the absence of dimorphic transition even when the level of residual glucose exceeded the threshold value. Further studies are needed to decipher the mechanism, nevertheless this work has clearly demonstrated that the dimorphic transition in *Y. lipolytica* is much more controlled by a sugar signaling pathway, most probably via cAMP-PKA-type signaling pathway, than by the pH or by DO responses. The responses to both stressors (pH and DO) were indeed clearly different depending on the residual glucose concentration in the medium.

Filamentation greatly impacts the rheological behavior of the fermentation broth, and transfer phenomena inside bioreactors and consequently bioprocess performance. Being able to control dimorphic transition via a fine control of the residual glucose level in the bioreactor based on well-controlled feeding strategy could be a relevant lever for bioprocess development.

Formatting of funding sources

This research did not receive any specific grant from funding agencies in the public, commercial, or not-for-profit sectors.

References

[1] Fickers P, Benetti PH, Wache Y, Marty A, Mauersberger S, Smit MS, et al. Hydrophobic substrate utilisation by the yeast *Yarrowia lipolytica*, and its potential applications. Fems Yeast Res 2005;5:527-543. doi: 10.1016/j.femsyr.2004.09.004

[2] Finogenova TV, Kamzolova SV, Dedyukhina EG, Shishkanova NV, Il'chenko AP, Morgunov IG, et al. Biosynthesis of citric and isocitric acids from ethanol by mutant *Yarrowia lipolytica* N 1 under continuous cultivation. Appl Microbiol Biot 2002;59:493-500. doi: 10.1007/s00253-002-1022-8

[3] Papanikolaou S, Galiotou-Panayotou M, Chevalot I, Komaitis M, Marc I, Aggelis G. Influence of glucose and saturated free-fatty acid mixtures on citric acid and lipid production by *Yarrowia lipolytica*. Curr Microbiol 2006;52:134-142. doi: 10.1007/s00284-005-0223-7

[4] Makri A, Fakas S, Aggelis G. Metabolic activities of biotechnological interest in *Yarrowia lipolytica* grown on glycerol in repeated batch cultures. Bioresource Technol 2010;101:2351-2358. doi: 10.1016/j.biortech.2009.11.024

[5] Sarris D, Galiotou-Panayotou M, Koutinas AA, Komaitis M, Papanikolaou S. Citric acid, biomass and cellular lipid production by *Yarrowia lipolytica* strains cultivated on olive mill wastewater-based media. J Chem Technol Biot 2011;86:1439-1448. doi: 10.1002/jctb.2658

[6] Coelho MAZ, Amaral PFF, Belo I. *Yarrowia lipolytica*: an industrial workhorse Current Research, Technology and Education Topics in Applied Microbiology and Microbial Biotechnology Advances 2010:930-940

[7] Bussamara R, Fuentefria AM, de Oliveira ES, Broetto L, Simcikova M, Valente P, et al. Isolation of a lipase-secreting yeast for enzyme production in a pilot-plant scale batch fermentation. Bioresource Technol 2010;101:268-275. doi: 10.1016/j.biortech.2008.10.063

[8] Madzak C, Gaillardin C, Beckerich JM. Heterologous protein expression and secretion in the non-conventional yeast *Yarrowia lipolytica*: a review. J Biotechnol 2004;109:63-81. doi: 10.1016/j.jbiotec.2003.10.027

[9] Papanikolaou S, Chevalot I, Galiotou-Panayotou M, Komaitis M, Marc I, Aggelis G. Industrial derivative of tallow: a promising renewable substrate for microbial lipid, single-cell protein and lipase production by *Yarrowia lipolytica*. Electron J Biotechn 2007;10:425-435. doi: 10.2225/vol10-issue3-fulltext-8

[10] Papanikolaou S, Chatzifragkou A, Fakas S, Galiotou-Panayotou M, Komaitis M, Nicaud J-M, et al. Biosynthesis of lipids and organic acids by *Yarrowia lipolytica* strains cultivated on glucose. Eur J Lipid Sci Tech 2009;111:1221-1232. doi: 10.1002/ejlt.200900055

[11] Parfene G, Horincar V, Tyagi AK, Malik A, Bahrim G. Production of medium chain saturated fatty acids with enhanced antimicrobial activity from crude coconut fat by solid state cultivation of *Yarrowia lipolytica*. Food Chem 2013;136:1345-1349. doi: 10.1016/j.foodchem.2012.09.057

[12] Timoumi A, Guillouet SE, Molina-Jouve C, Fillaudeau L, Gorret N. Impacts of environmental conditions on product formation and morphology of *Yarrowia lipolytica*. Appl Microbiol Biotechnol 2018;102:3831-3848. doi: 10.1007/s00253-018-8870-3

[13] Timoumi A, Bideaux C, Guillouet SE, Allouche Y, Molina-Jouve C, Fillaudeau L, et al. Influence of oxygen availability on the metabolism and morphology of *Yarrowia lipolytica*: insights into the impact of glucose levels on dimorphism. Appl Microbiol Biotechnol 2017; 101:7317-7333. doi: 10.1007/s00253-017-8446-7

[14] Timoumi A, Cleret M, Bideaux C, Guillouet SE, Allouche Y, Molina-Jouve C, et al. Dynamic behavior of *Yarrowia lipolytica* in response to pH perturbations: dependence

of the stress response on the culture mode. Appl Microbiol Biotechnol 2017;101:351-366. doi: 10.1007/s00253-016-7856-2

[15] Bellou S, Makri A, Triantaphyllidou IE, Papanikolaou S, Aggelis G. Morphological and metabolic shifts of *Yarrowia lipolytica* induced by alteration of the dissolved oxygen concentration in the growth environment. Microbiol-SGM 2014;160:807-817. doi: 10.1099/mic.0.074302-0

[16] Cervantes-Chavez JA, Kronberg F, Passeron S, Ruiz-Herrera J. Regulatory role of the PKA pathway in dimorphism and mating in *Yarrowia lipolytica*. Fungal Genet Biol 2009;46:390-399. doi: 10.1016/j.fgb.2009.02.005

[17] Cervantes-Chavez JA, Ruiz-Herrera J. STE11 disruption reveals the central role of a MAPK pathway in dimorphism and mating in *Yarrowia lipolytica*. Fems Yeast Res 2006;6:801-815. doi: 10.1111/j.1567-1364.2006.00084.x

[18] Cervantes-Chavez JA, Ruiz-Herrera J. The regulatory subunit of protein kinase A promotes hyphal growth and plays an essential role in *Yarrowia lipolytica*. Fems Yeast Res 2007;7:929-940. doi: 10.1111/j.1567-1364.2007.00265.x

[19] Ruiz-Herrera J, Sentandreu R. Different effectors of dimorphism in *Yarrowia lipolytica*. Arch Microbiol 2002;178:477-483. doi: 10.1007/s00203-002-0478-3

[20] Hurtado CAR, Beckerich JM, Gaillardin C, Rachubinski RA. A Rac homolog is required for induction of hyphal growth in the dimorphic yeast *Yarrowia lipolytica*. J Bacteriol 2000;182:2376-2386. doi: 10.1128/jb.182.9.2376-2386.2000

[21] Topiltin Morales-Vargas A, Dominguez A, Ruiz-Herrera J. Identification of dimorphism-involved genes of *Yarrowia lipolytica* by means of microarray analysis. Res Microbiol 2012;163:378-387. doi: 10.1016/j.resmic.2012.03.002

[22] Martinez-Vazquez A, Gonzalez-Hernandez A, Dominguez A, Rachubinski R, Riquelme M, Cuellar-Mata P, et al. Identification of the Transcription Factor Znc1p, which Regulates the Yeast-to-Hypha Transition in the Dimorphic Yeast *Yarrowia lipolytica*. Plos One 2013;8. doi: 10.1371/journal.pone.0066790

[23] Morin M, Monteoliva L, Insenser M, Gil C, Dominguez A. Proteomic analysis reveals metabolic changes during yeast to hypha transition in *Yarrowia lipolytica*. J Mass Spectrom 2007;42:1453-1462. doi: 10.1002/jms.1284

[24] Buu L-M, Chen Y-C. Impact of glucose levels on expression of hypha-associated secreted aspartyl proteinases in Candida albicans. J Biomed Sci 2014;21:22-22. doi: 10.1186/1423-0127-21-22

[25] Laurian R, Dementhon K, Doumèche B, Soulard A, Noel T, Lemaire M, et al. Hexokinase and Glucokinases Are Essential for Fitness and Virulence in the Pathogenic Yeast Candida albicans. Front Microbiol 2019;10. doi: 10.3389/fmicb.2019.00327

[26] Van de Velde S, Thevelein JM. Cyclic AMP-protein kinase A and Snf1 signaling mechanisms underlie the superior potency of sucrose for induction of filamentation in Saccharomyces cerevisiae. Eukaryot Cell 2008;7:286-293. doi: 10.1128/EC.00276-07

[27] Johnson C, Kweon HK, Sheidy D, Shively CA, Mellacheruvu D, Nesvizhskii AI, et al. The yeast Sks1p kinase signaling network regulates pseudohyphal growth and glucose response. PLoS Genet 2014;10:e1004183-e1004183. doi: 10.1371/journal.pgen.1004183

[28] Rødkær SV, Færgeman NJ. Glucose- and nitrogen sensing and regulatory mechanisms in Saccharomyces cerevisiae. FEMS Yeast Res 2014;14:683-696. doi: 10.1111/1567-1364.12157

[29] Rolland F, Winderickx J, Thevelein JM. Glucose-sensing and -signalling mechanisms in yeast. FEMS Yeast Res 2002;2:183-201. doi: 10.1111/j.1567-1364.2002.tb00084.x

513 [30] Santangelo GM. Glucose signaling in Saccharomyces cerevisiae. Microbiol Mol Biol
514 Rev 2006;70:253-282. doi: 10.1128/MMBR.70.1.253-282.2006
515 [31] Sabina J, Brown V. Glucose sensing network in Candida albicans: a sweet spot for
516 fungal morphogenesis. Eukaryot Cell 2009;8:1314-1320. doi: 10.1128/EC.00138-09
517 [32] Zaman S, Lippman SI, Schneper L, Slonim N, Broach JR. Glucose regulates
518 transcription in yeast through a network of signaling pathways. Mol Syst Biol
519 2009;5:245-245.
520 doi: 10.1038/msb.2009.2
521 [33] Kuttykrishnan S, Sabina J, Langton LL, Johnston M, Brent MR. A quantitative model of
522 glucose signaling in yeast reveals an incoherent feed forward loop leading to a
523 specific, transient pulse of transcription. P Natl Acad Sci USA 2010;107:16743-
524 16748.
525 doi: 10.1073/pnas.0912483107
526 [34] Kim J-H, Roy A, Jouandot D, Cho KH. The glucose signaling network in yeast.
527 2013;1830:5204-5210. https://doi.org/10.1016/j.bbagen.2013.07.025
528 [35] Roy A, Kim YB, Cho KH, Kim JH. Glucose starvation-induced turnover of the yeast
529 glucose transporter Hxt1. Biochim Biophys Acta 2014;1840:2878-2885.
530 doi: 10.1016/j.bbagen.2014.05.004
531 [36] Cairey-Remonnay A, Deffaud J, Wésolowski-Louvel M, Lemaire M, Soulard A.
532 Glycolysis controls plasma membrane glucose sensors to promote glucose signaling in
533 yeasts. Mol Cell Biol 2015;35:747-757. doi: 10.1128/MCB.00515-14
534 [37] Lazar Z, Neuvéglise C, Rossignol T, Devillers H, Morin N, Robak M, et al.
535 Characterization of hexose transporters in Yarrowia lipolytica reveals new groups of
536 Sugar Porters involved in yeast growth. Fungal Genet Biol 2017;100:1-12.
537 https://doi.org/10.1016/j.fgb.2017.01.001
538 [38] Lee KS, Ram RJ. Plastic–PDMS bonding for high pressure hydrolytically stable active
539 microfluidics. Lab Chip 2009;9:1618-1624. doi: 10.1039/B820924C
540 [39] Lee KS, Boccazzi P, Sinskey AJ, Ram RJ. Microfluidic chemostat and turbidostat with
541 flow rate, oxygen, and temperature control for dynamic continuous culture. Lab Chip
542 2011;11:1730-1739. doi: 10.1039/C1LC20019D
543 [40] Bower DM, Lee KS, Ram RJ, Prather KLJ. Fed-batch microbioreactor platform for scale
544 down and analysis of a plasmid DNA production process. Biotechnol Bioeng
545 2012;109:1976-1986. doi: 10.1002/bit.24498
546 [41] Torres-Guzmán JC, Domínguez A. HOY1, a homeo gene required for hyphal formation
547 in Yarrowia lipolytica. Mol Cell Biol 1997;17:6283-6293. doi:
548 10.1128/mcb.17.11.6283
549 [42] Hurtado CA, Rachubinski RA. MHY1 encodes a C2H2-type zinc finger protein that
550 promotes dimorphic transition in the yeast Yarrowia lipolytica. J Bacteriol
551 1999;181:3051-3057. doi: 10.1128/JB.181.10.3051-3057.1999
552 [43] Gonzalez-Lopez CI, Ortiz-Castellanos L, Ruiz-Herrera J. The ambient pH response Rim
553 pathway in *Yarrowia lipolytica*: Identification of YlRIM9 and characterization of its
554 role in dimorphism. Curr Microbiol 2006;53:8-12. doi: 10.1007/s00284-005-0070-6
555 [44] Kronberg F, Giacometti R, Ruiz-Herrera J, Passeron S. Characterization of the regulatory
556 subunit of Yarrowia lipolytica cAMP-dependent protein kinase. Evidences of a
557 monomeric protein. Arch Biochem Biophys 2011;509:66-75.
558 doi: 10.1016/j.abb.2011.03.001
559 [45] Morales-Vargas AT, Dominguez A, Ruiz-Herrera J. Identification of dimorphism-
560 involved genes of *Yarrowia lipolytica* by means of microarray analysis. Res Microbiol
561 2012;163:378-387. doi: 10.1016/j.resmic.2012.03.002

562 [46] Liang SH, Wu H, Wang RR, Wang Q, Shu T, Gao XD. The TORC1-Sch9-Rim15
563 signaling pathway represses yeast-to-hypha transition in response to glycerol
564 availability in the oleaginous yeast Yarrowia lipolytica. Mol Microbiol 2017;104:553-
565 567.
566 doi: 10.1111/mmi.13645
567 [47] Pomraning KR, Bredeweg EL, Kerkhoven EJ, Barry K, Haridas S, Hundley H, et al.
568 Regulation of Yeast-to-Hyphae Transition in Yarrowia lipolytica. mSphere
569 2018;3:e00541-00518. doi: 10.1128/mSphere.00541-18
570 [48] Li M, Li YQ, Zhao XF, Gao XD. Roles of the three Ras proteins in the regulation of
571 dimorphic transition in the yeast Yarrowia lipolytica. FEMS Yeast Res 2014;14:451-
572 463. doi: 10.1111/1567-1364.12129
573 [49] Lengeler KB, Davidson RC, D'Souza C, Harashima T, Shen WC, Wang P, et al. Signal
574 transduction cascades regulating fungal development and virulence. Microbiol Mol
575 Biol Rev 2000;64:746-785. doi: 10.1128/mmbr.64.4.746-785.2000
576 [50] Borges-Walmsley MI, Walmsley AR. cAMP signalling in pathogenic fungi: control of
577 dimorphic switching and pathogenicity. Trends Microbiol 2000;8:133-
578 141.https://doi.org/10.1016/S0966-842X(00)01698-X
579 [51] Pollack JH, Hashimoto T. The Role of Glucose in the pH Regulation of Germ-tube
580 Formation in Candida albicans. Microbiology 1987;133:415-
581 424.https://doi.org/10.1099/00221287-133-2-415
582 [52] Bruatto M, Gremmi M, Nardacchione A, Amerio M. Effect of glucose starvation on
583 germ-tube production by Candida albicans. Mycopathologia 1993;123:105-110.
584 doi: 10.1007/bf01365088
585 [53] Spagnuolo M, Shabbir Hussain M, Gambill L, Blenner M. Alternative Substrate
586 Metabolism in Yarrowia lipolytica. Front Microbiol 2018;9:1077. doi:
587 10.3389/fmicb.2018.01077

588

589

Figure captions

Fig. 1: Picture of the two experimental designs. **A.** Conventional 1L-labscale bioreactor, **B.** 1mL-microfluidic bioreactor.

Fig. 2: Dynamic evolution of pH, DO, dilution rate, biomass and residual glucose concentration during the steady state and accelerostat phases of the 1-L bioreactor culture: (×) pH, (Δ) DO level, black line (—) dilution rate, (o) Biomass, (•) Residual glucose concentration.

Fig. 3: Effect of residual glucose concentration on the physiological states of *Y. lipolytica* populations cultivated under accelerostat mode in 1L-labscale bioreactor culture. **A.** Dynamic evolution of the filamentous subpopulation, in volume (o), and residual glucose concentration (•) during the accelerostat. **B.** Box plots comparing the time-evolution of length distribution measurements for cells under under chemostat and accelerostat modes (data quantified by flow cytometry). The lower boundary of the box indicates the 25^{th} percentile, a black line marks the median, a red line marks the mean and the upper boundary of the box indicates the 75^{th} percentile. Whiskers above and below the box indicate the 90^{th} and 10^{th} percentiles. The black dots indicate the 95^{th} and 5^{th} percentiles. **C.** Light micrographs showing morphological changes of *Y. lipolytica* W29 in response to the increase of dilution rate under accelerostat modes. As growth progressed, observations were performed using a light microscope, without oil fixation, and at magnifications of 40 x.

Fig. 4: Dynamic evolutions of pH, DO, dilution rate, biomass and residual glucose concentration during the steady state and accelerostat phases of the 1mL-microfluidic bioreactor cultures: (×) pH, (Δ) DO level, black line (—) dilution rate, (o) biomass, (•) residual glucose concentration.

Fig. 5: Effect of residual glucose concentration on the physiological states of *Y. lipolytica* populations cultivated under accelerostat mode in 1mL-microfluidic bioreactor. **A.** Dynamic evolution of the filamentous subpopulation, in volume (o), and Residual glucose concentration (•) during the accelerostat without cAMP supplementation. **B.** Box plots comparing the time-evolution of length distribution measurements for cells under under accelerostat modes with and without cAMP supplementation (data quantified by flow cytometry). The lower boundary of the box indicates the 25^{th} percentile, a black line marks

620 the median, a red line marks the mean and the upper boundary of the box indicates the 75th
621 percentile. Whiskers above and below the box indicate the 90th and 10th percentiles. The black
622 dots indicate the 95th and 5th percentiles. **C.** Light micrographs showing morphological
623 changes of *Y. lipolytica* W29 in response the increase of residual glucose during accelerostat
624 without cAMP. As growth progressed, observations were performed using a light microscope,
625 without oil fixation, and at magnifications of 40 x.

626 **Fig. 6:** Dynamic evolutions of cAMP intracellular concentration during the steady state and
627 accelerostat phases with and without cAMP of the 1mL-microfluidic and 1L- bioreactor.

A

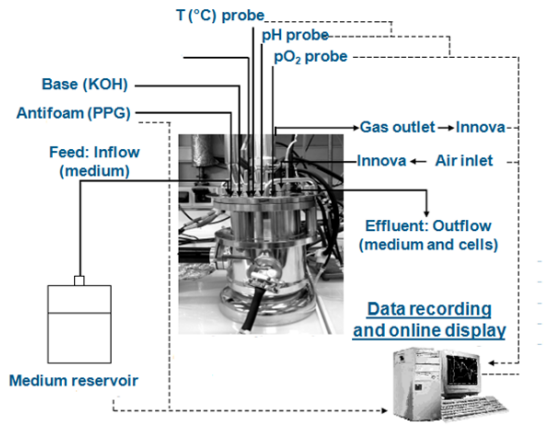

- **1L - lab-scale bioreactor**
- Accelerostat mode (ACC): D= 0.12 to 0.24 h^{-1}
- Culture without cAMP
- pH stress: Chemostat vs ACC at pH5.6

B

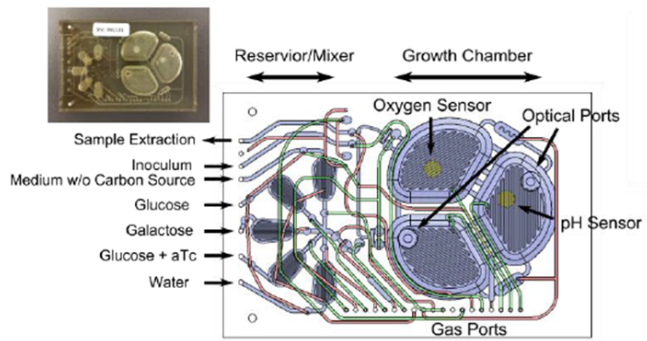

- **Single-use 1mL - microreactor**
- Mode Accelerostat: D=0.15 to 0.24 h^{-1}
- Culture with and without cAMP
- pH stress: Chemostat vs ACC at pH5.6

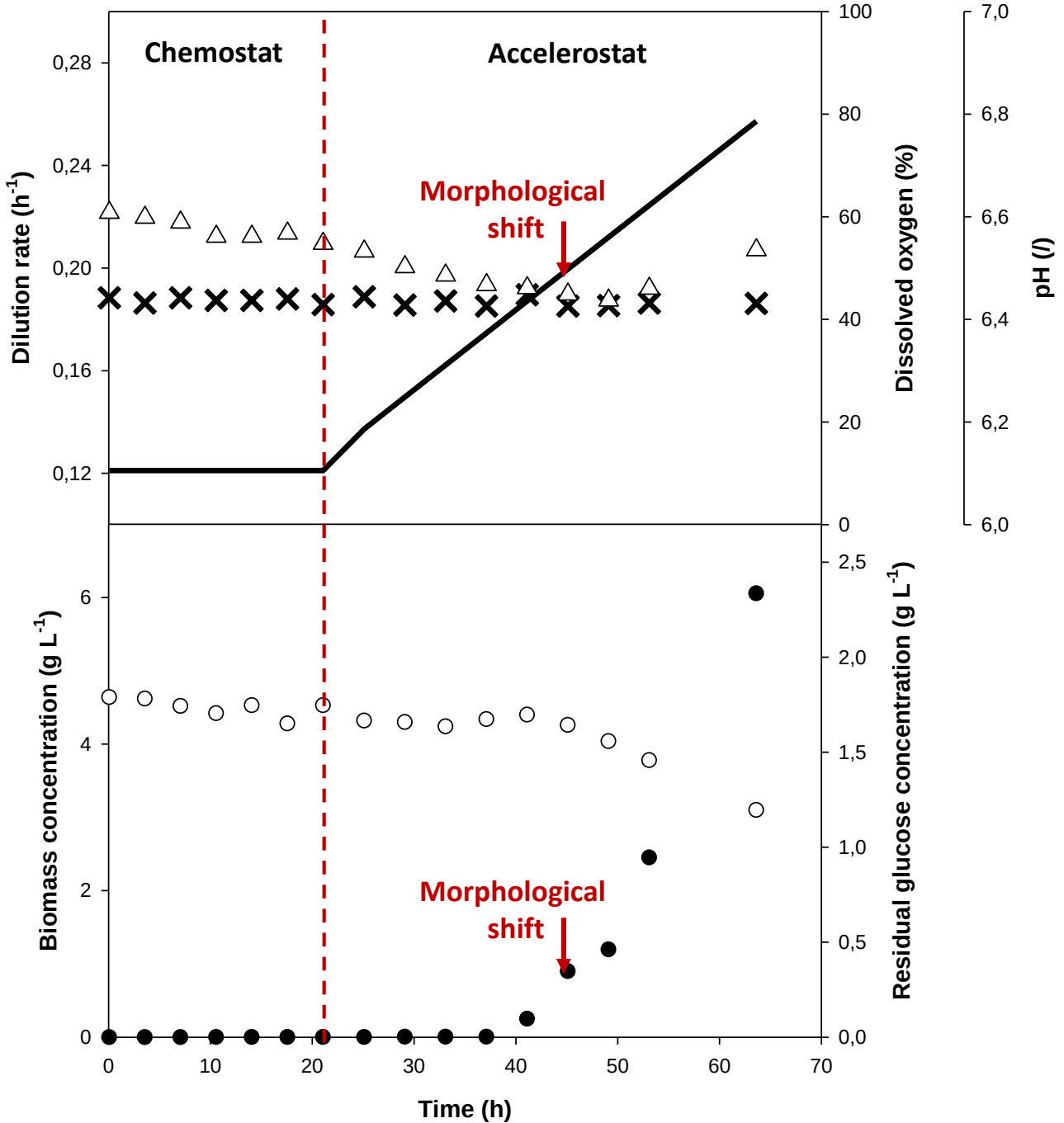
Chemostat
Accelerostat
Morphological shift
Morphological shift
Dilution rate (h-1)
Dissolved oxygen (%)
pH (/)
Biomass concentration (g L-1)
Residual glucose concentration (g L-1)
Time (h)
0,28
0,24
0,20
0,16
0,12
100
80
60
40
20
0
7,0
6,8
6,6
6,4
6,2
6,0
6
4
2
0
2,5
2,0
1,5
1,0
0,5
0,0
0
10
20
30
40
50
60
70

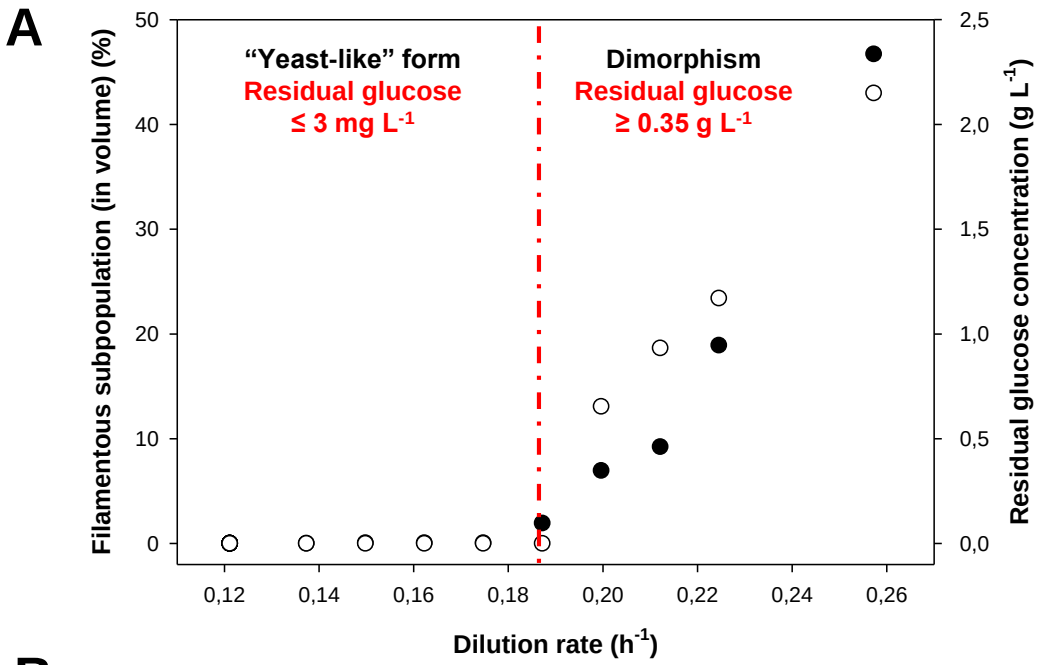
A
"Yeast-like" form
Residual glucose
≤ 3 mg L-1
Dimorphism
Residual glucose
≥ 0.35 g L-1
Filamentous subpopulation (in volume) (%)
Residual glucose concentration (g L-1)
Dilution rate (h-1)
50
40
30
20
10
0
2,5
2,0
1,5
1,0
0,5
0,0
0,12
0,14
0,16
0,18
0,20
0,22
0,24
0,26

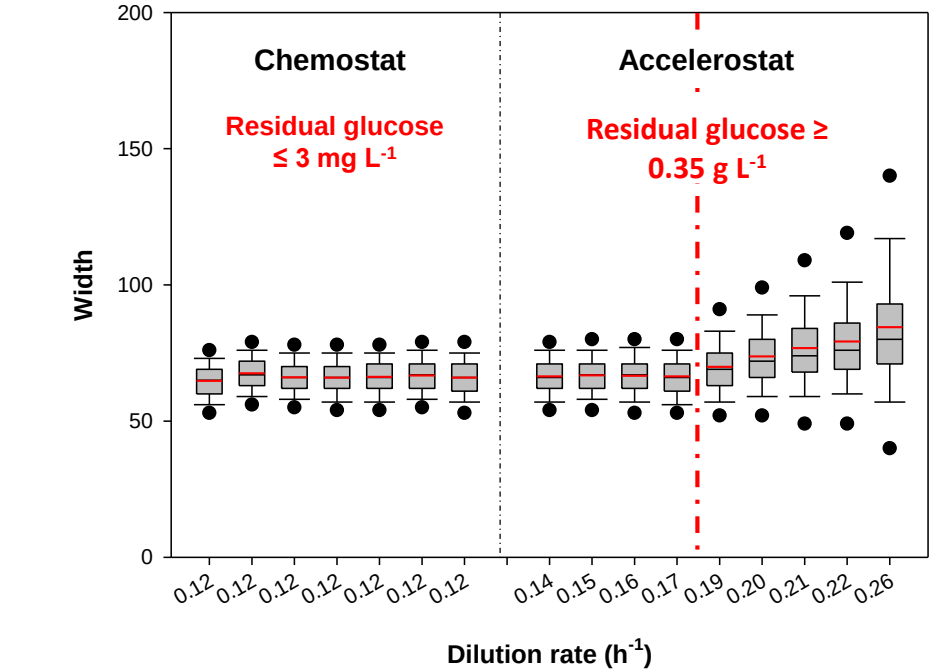
B
Chemostat
Residual glucose
≤ 3 mg L-1
Accelerostat
Residual glucose ≥
0.35 g L-1
Width
Dilution rate (h-1)
200
150
100
50
0
0.12
0.12
0.12
0.12
0.12
0.12
0.12
0.14
0.15
0.16
0.17
0.19
0.20
0.21
0.22
0.26

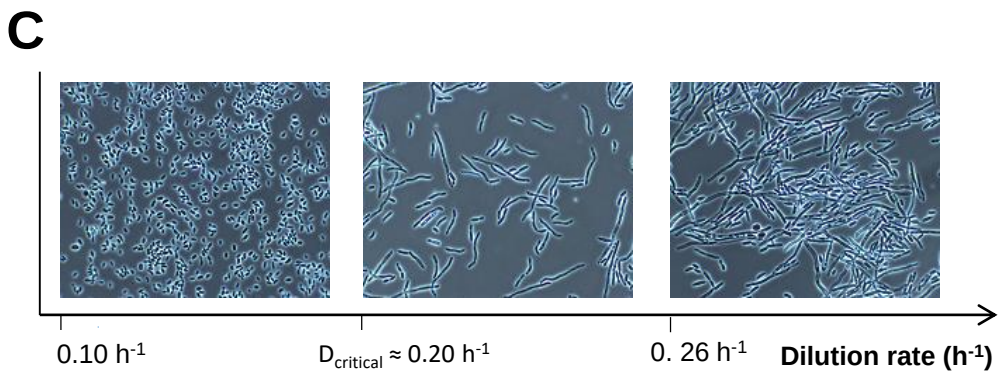
C
0.10 h-1
Dcritical ≈ 0.20 h-1
0. 26 h-1
Dilution rate (h-1)

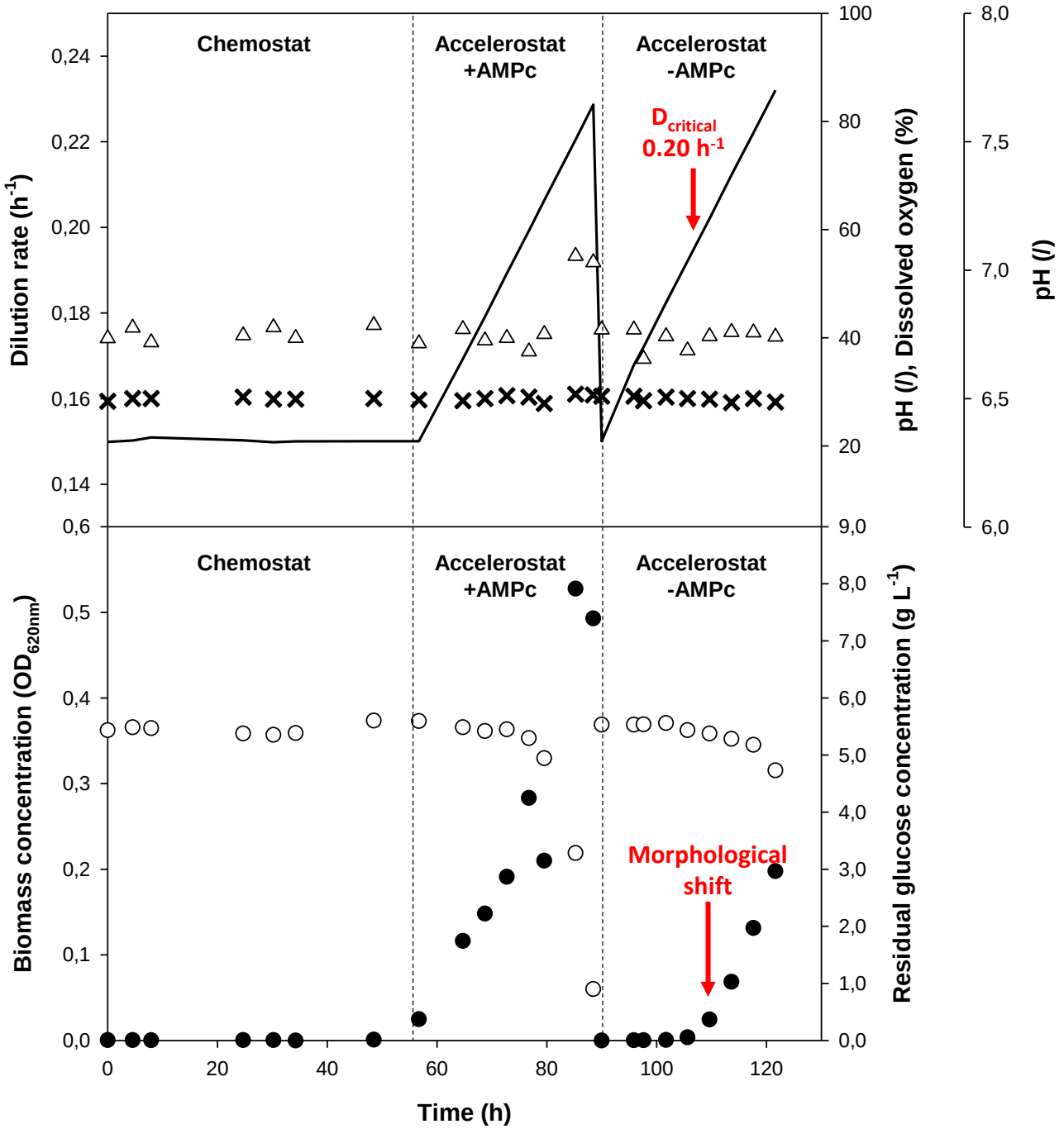
Chemostat
Accelerostat +AMPc
Accelerostat -AMPc
$D_{critical}$ 0.20 h^{-1}
Dilution rate (h^{-1})
pH (/), Dissolved oxygen (%)
pH (/)
Chemostat
Accelerostat +AMPc
Accelerostat -AMPc
Morphological shift
Biomass concentration (OD_{620nm})
Residual glucose concentration (g L^{-1})
Time (h)

A

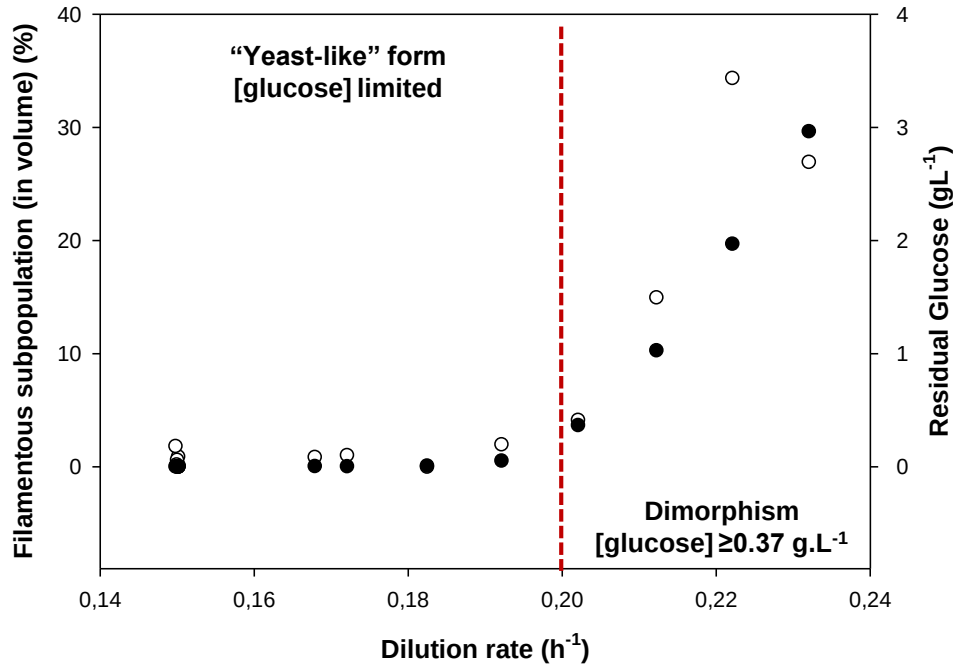

B

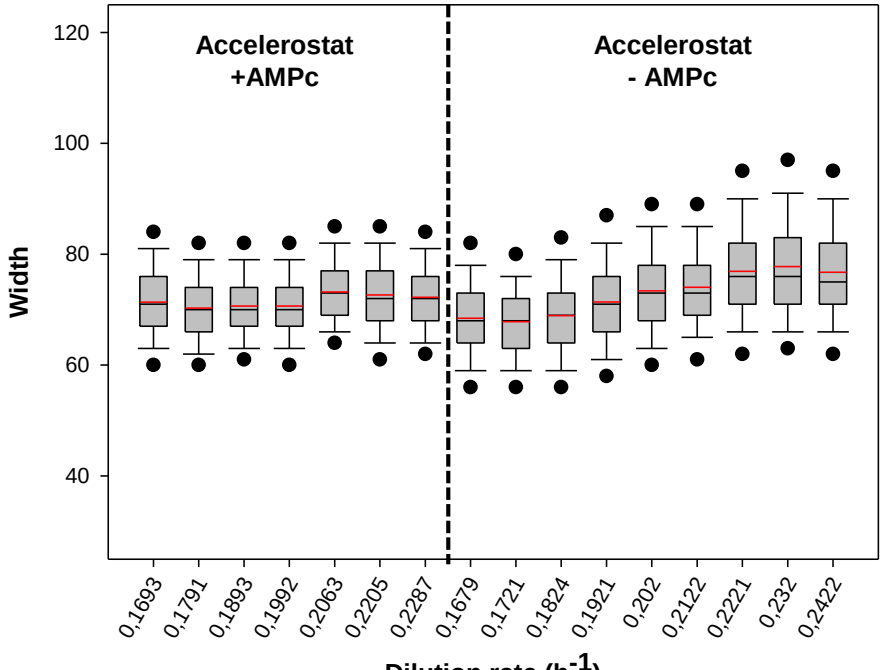

C

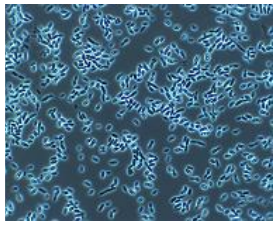

"Yeast-like" form
∀ D and
[Glucose] limited

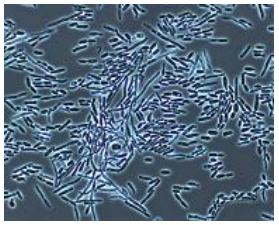

Dimorphism
[Glucose] ≥ 0.37 gL^{-1}
$D_{critical} \approx 0.20\ h^{-1}$

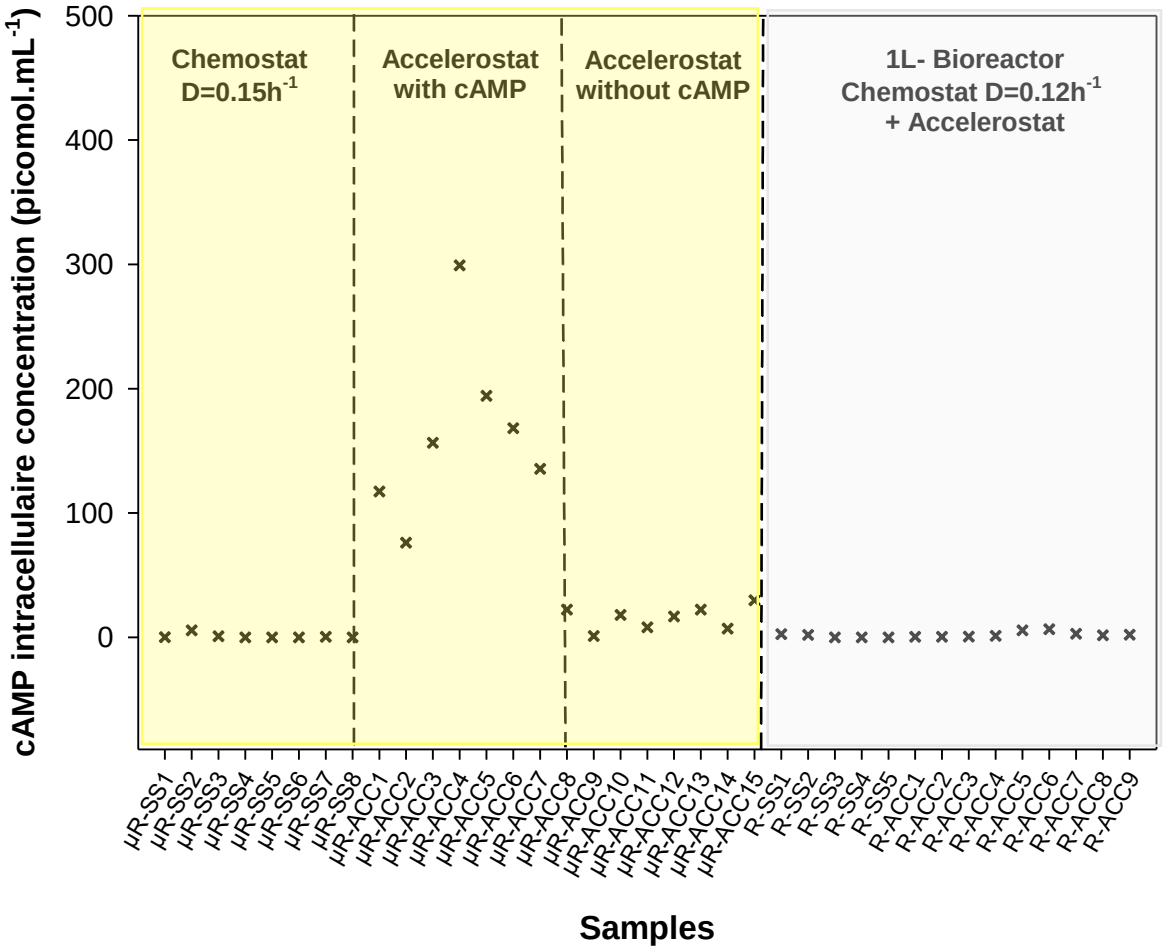
cAMP intracellulaire concentration (picomol.mL-1)
500
400
300
200
100
0
Chemostat
D=0.15h-1
Accelerostat
with cAMP
Accelerostat
without cAMP
1L- Bioreactor
Chemostat D=0.12h-1
+ Accelerostat
µR-SS1
µR-SS2
µR-SS3
µR-SS4
µR-SS5
µR-SS6
µR-SS7
µR-SS8
µR-ACC1
µR-ACC2
µR-ACC3
µR-ACC4
µR-ACC5
µR-ACC6
µR-ACC7
µR-ACC8
µR-ACC9
µR-ACC10
µR-ACC11
µR-ACC12
µR-ACC13
µR-ACC14
µR-ACC15
R-SS1
R-SS2
R-SS3
R-SS4
R-SS5
R-ACC1
R-ACC2
R-ACC3
R-ACC4
R-ACC5
R-ACC6
R-ACC7
R-ACC8
R-ACC9
Samples

Table 1. Kinetic parameters of the continuous cultures during the steady-state phase: Average values of specific rates, yields, respiratory quotients, carbon and redox recoveries were expressed with their associated standard deviations

Dilution rate	pH	-qS	qCO_2	$-qO_2$	$Y_{X/S}$	RQ_{mean}	Carbon recovery	Redox recovery	Reference
(h^{-1})		(Cmol $CmolX^{-1}$ h^{-1})			(Cmol $Cmol^{-1}$)	(/)	(%)		
0.10	pH 7	0.160±0.001	0.053±0.010	0.044±0.003	0.65±0.01	1.10±0.05	97.4±1.3	100.6±0.8	[14]
0.12	pH 6.5	0.194±0.002	0.081±0.006	0.073±0.005	0.61±0.01	1.11±0.01	103±4	105±6	This work